MASTER

RFP-933

$2 73
7/6/67

TENSILE PROPERTIES OF GAMMA QUENCHED AND AGED URANIUM-RICH NIOBIUM ALLOYS

BY ROSS J. JACKSON, RONALD P. BRUGGER, AND DELMAR V. MILEY

THE DOW CHEMICAL COMPANY
ROCKY FLATS DIVISION
P. O. BOX 888
GOLDEN, COLORADO 80401
U.S. ATOMIC ENERGY COMMISSION
CONTRACT AT(29-1)-1106

Printed in USA. Price $ 3 Available from the Clearinghouse for Federal
Scientific and Technical Information, National Bureau of Standards
U. S. Department of Commerce, Springfield, Virginia. 22151

2 June 1967

RFP-933
UC-25 METALS, CERAMICS,
AND MATERIALS
TID-4500

CFSTI PRICES

H.C. $3.00; MN 65

TENSILE PROPERTIES OF GAMMA QUENCHED AND AGED URANIUM-RICH NIOBIUM ALLOYS

BY ROSS J. JACKSON, RONALD P. BRUGGER, AND DELMAR V. MILEY

THE DOW CHEMICAL COMPANY
ROCKY FLATS DIVISION
P. O. BOX 888
GOLDEN, COLORADO 80401
U. S. ATOMIC ENERGY COMMISSION
CONTRACT AT(29-1)-1106

TENSILE PROPERTIES OF GAMMA QUENCHED AND AGED URANIUM-RICH NIOBIUM ALLOYS

BY ROSS J. JACKSON, RONALD P. BRUGGER, AND DELMAR V. MILEY

Tensile-test data are presented for uranium-rich niobium alloys containing 11, 15, 17, and 19 a/o niobium in both the solution-quenched and the aged conditions. The tensile-test data are correlated with concurrent metallographic and x-ray studies. The results show that a wide variety of mechanical properties are available from these heat-treatable, corrosion-resistant, high-density alloys.

Introduction

The investigation of the uranium-niobium system was undertaken as part of a general program to find a uranium-rich alloy possessing: (a) corrosion resistance properties, (b) heat-treating characteristics leading to favorable mechanical properties, (c) formability, (d) dimensional stability, (e) low neutron capture cross-section, and (f) high density.

A search of open literature revealed a number of significant research studies dealing with uranium-niobium alloys. A number of uranium-niobium equilibrium diagrams have been reported.[1-5] Other aspects of the system such as phase stability and decomposition,[6-8] metastable phases,[9,10] and diffusion[11,12] have been investigated.

Unfortunately, none of the reported studies are concerned with the mechanical properties of the uranium-niobium system. It is the intent of this work to investigate mechanical properties as a function of heat treatments, and to determine the optimum tensile properties commensurate with a given application.

Experimental

Materials.—The uranium was magnesium-reduced derby material. The niobium was sintered material rolled to 120-mil strip. A partial chemical analysis of both metals is given in Table I.

Alloy Preparation.—The component metals were fabricated into box electrodes. These were arc-melted in a consummable-electrode arc furnace into a water-cooled copper mold. The ingots were then inverted

TABLE I

CHEMICAL ANALYSIS OF CONSTITUENT METALS AND THEIR ALLOYS

Element	Niobium* (ppm)	Uranium (ppm)	Arc-cast alloy	Induction re-cast alloy
Al	< 20	10	<10	<10
As	< 50			
B	< 10		< 1	< 1
Ba			<50	<50
Be	< 10		< 1	<10
Bi	< 10		<10	<10
C	40	50	90	140
Ca	<100		<50	<50
Cd	< 10		<10	<10
Co	< 10		<10	<10
Cr	< 20		<50	<50
Cu	< 20		7	8
Fe	10	30	50	60
Ge	< 10			
H	4			
Hg	< 10			
K	< 10		< 1	< 1
Li	< 10		< 1	< 1
Mg			<10	<10
Mn	< 10		<10	<10
Mo	15		<10	<10
N	50			
Ni	10		<10	<10
O	80			
Pb	< 10		< 1	< 1
Sb	< 10			<10
Si	< 10	30	20	30
Sn	< 10		<10	<10
Ta	250			
Ti	< 50		<50	<50
V	<100		<10	<10
W	50			
Zn			<50	<50
Zr	<100			

* Brinell hardness number of 52

---

(1) B. Sawyer, "Uranium-Columbium Alloy System." Argonne National Laboratory, 1946, ANL-4027.

(2) B. A. Rogers, D. F. Atkins, E. J. Manthos, and M. E. Kirkpatrick, *Trans. Met. Soc. AIME, 212*, 387-393 (1957).

(3) A. E. Dwight and M. H. Mueller, "Constitution of the Uranium-Rich U-Nb and U-Nb-Zr Systems," Argonne National Laboratory, 1957, ANL-5581.

(4) P. C. L. Pfeil, J. D. Browne, and G. K. Williamson, *J. Inst. Metals, 87*, 204-208 (1959).

(5) O. S. Ivanov and G. I. Terekhov, "Structure of Alloys of Certain Systems Containing Uranium and Thorium," E. M. Potapova, ed., Academy of Sciences USSR, 1961, U.S. AEC Translation, 1963, AEC-tr-5834.

(6) O. S. Ivanov and Yu. S. Virgiliev, *J. Nucl. Materials, 6*, 199-202 (1962).

(7) C. A. W. Peterson, "Study of the Isothermal Transformations of Some Binary Uranium-Base Alloys Between 400°C and 650°C," Lawrence Radiation Laboratory, 1964, UCRL-7824.

(8) C. D'Amato, F. S. Saraceno and T. B. Wilson, *J. Nucl. Materials, 12*, 291-304 (1964).

(9) K. Tangri and D. K. Chaudhuri, *J. Nucl. Materials, 15*, 278-287 (1964).

(10) M. Anagnostidis, M. Colombie et H. Monti, *J. Nucl. Materials, 11*, 67-76 (1964).

(11) N. L. Peterson and R. E. Ogilvie, *Trans. Met. Soc. AIME, 218*. 439-444 (1960).

(12) N. L. Peterson and R. E. Ogilvie, *Trans. Met. Soc. AIME, 227*, 1083-1087 (1963).

and again arc-melted. These double-arc-cast ingots were homogenized for 2 hours at 1100°C. This material was then hot rolled to sheet from which the tensile-test blanks were cut. A partial chemical analysis of the double arc-cast alloy is given in Table I.

In some instances the rolled, double arc-cast alloy was induction re-cast into bar stock, re-homogenized 2 hours at 1100°C, and then hot rolled to rods from which the tensile-test blanks were cut. The induction cast alloy generally had a higher inclusion content and an apparent lower niobium content (approximately 0.5 w/o niobium) than the starting arc-cast material. A partial chemical analysis of this material is listed in Table I.

Tensile Test Bar Preparation, Heat Treating and Testing Procedure.—Two types of tensile test bars were used, and these bars conformed to the specifications shown in Figure 1. Flat specimens which were used in the majority of instances were cut from hot rolled, double arc-cast sheet material. The round bars were from hot rolled rods that were previously induction cast as described earlier. Before aging, the sheet and the rod blanks were heated 30 minutes at 850°C and then they were water quenched.

The blanks were aged for various periods of time and at various temperatures, air cooled to ambient temperature, and then machined. It was believed that this procedure would be similar to that of a production process. In some instances, however, the tensile samples were machined and then aged. In other instances the samples were machined, water quenched from 850°C, aged, and then tested. In some cases, after machining and heat treating, but before testing, the specimens were electropolished by the method described in RFP-862.[13] The reasons for the variations was to evaluate their effects on the resulting tensile properties.

Tensile tests were performed at room temperature in air on a Tinius-Olsen Model Super L tensile tester at a strain rate of 0.002 in./in./minute. Except where noted, two or three specimens were tested for each heat treatment. The hot tensile tests were conducted in a similar manner using a vertical-tube-furnace and an air atmosphere.

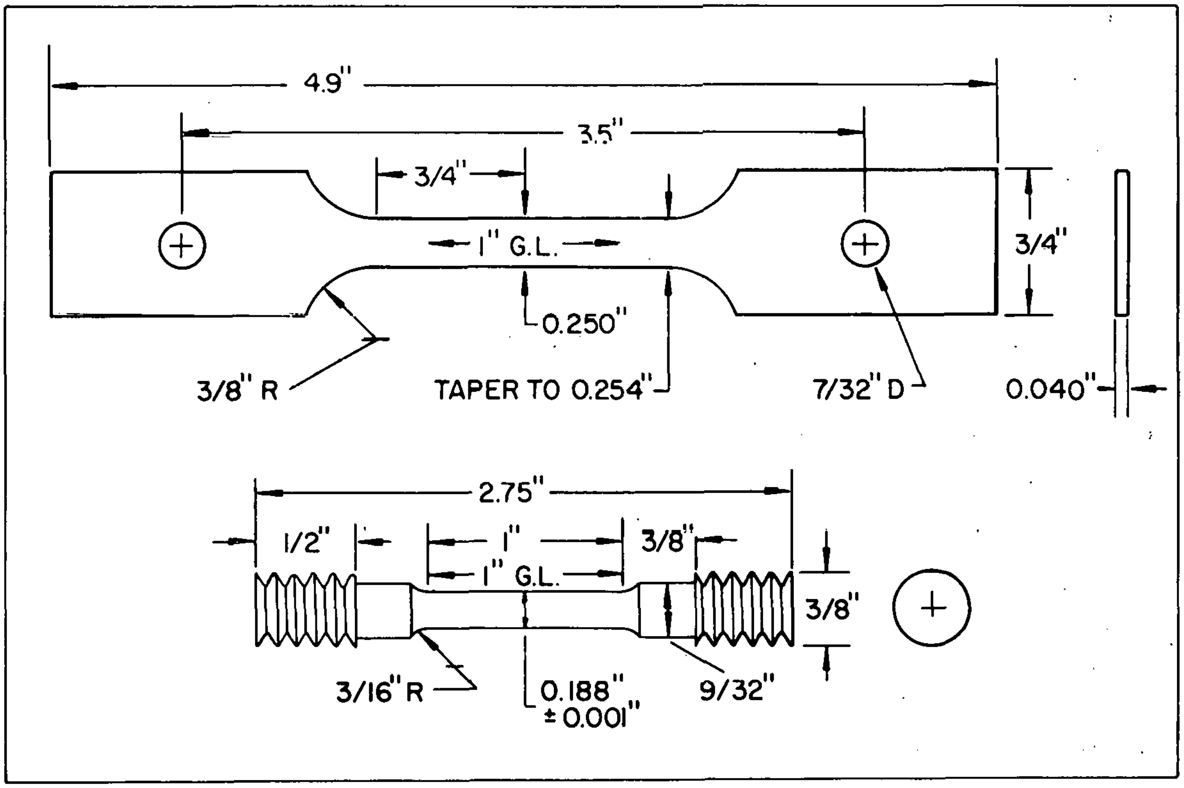

Figure 1.—Dimensional specifications for the flat plate and the round tensile-test specimens.

---

[13] R. J. Jackson, W. L. Johns, and A. E. Calabra, "Simplified Metallographic Technique for Uranium Alloys and Other Metals," The Dow Chemical Company, Rocky Flats Division, January 20, 1967, RFP-862.

Hardness measurements were taken of the grip area before testing the specimens. These values are an average of four readings. After fracture, longitudinal sections of selected specimens were metallographically examined. These same longitudinal sections then were subjected to x-ray examination using filtered CuKα radiation and a diffractometer.

Nomenclature.—A number of stable and metastable phases are observed in the composition range of interest. A resume of these phases is given in Table II. Microstructural connotations can be added to the phase designations using the subscripts a, b, c, d, g, and p; referring to acicular, banded, crosshatch, deformation bands, granular, and pearlitic connotations, respectively.

Data concerning the metastable phases and their hardness, as a function of phase-composition at various cooling rates from the gamma region, are shown in Figure 2. These data are from Anagnostidis *et al.*[14] Similar data have been presented by Tangri and Chaudhuri.[15]

Results

Presentation of Mechanical Data.—The mechanical test data are presented in five figures and two tables as follows:

Figure 3.—Test data for the quenched and aged uranium-11 a/o niobium alloy.

Figure 4.—Test data for the quenched and aged uranium-15 a/o niobium alloy.

Figure 5.—Test data for the quenched and aged uranium-19 a/o niobium alloy.

Figure 6.—Test data for the uranium-15 a/o niobium alloy aged for various times at 150°C.

Figure 7.—Hot tensile strengths of quenched and aged uranium-15 a/o niobium alloys.

Table III.—Supplementary mechanical test data presented in tabular form for the uranium-11 a/o niobium alloy.

Table IV.—Test data presented in tabular form for the uranium-17 a/o niobium alloy.

The mechanical test data for the quenched and aged 11, 15, and 19 a/o niobium alloys are shown in Figures 3, 4, and 5, respectively. The samples were all gamma-quenched flat bars cut from hot-rolled, arc-cast material. The aged samples were held one hour at the indicated temperature and air cooled, and then machined.

The shape of the curves for the three compositions are similar. In general, the alloys show a low strength and high ductility in the solution quenched condition. Aging at 350°C or lower results in a notable strengthening while maintaining reasonably good ductility properties. At 400° to 500°C the alloys develop a high strength and almost a complete loss of ductility. Aging above 525°C shows an improvement in ductility properties with a corresponding loss in strength.

In the high temperature aging experiments, the 550°C treatment yields the toughest material. Yield (0.2 percent offset) and ultimate tensile strengths of 160,000 psi and 200,000 psi, respectively, combined with reasonably good ductility properties are obtainable. The major disadvantage of this treatment is the

TABLE II

EQUILIBRIUM AND TRANSITION PHASES OBSERVED IN THE URANIUM-NIOBIUM SYSTEM

Symbol	Description	Crystal structure
α	Equilibrium α solid solution in stable or metastable form. Contains less than 1 a/o niobium.	Orthorhombic
β	Equilibrium β solid solution in stable or metastable form. Contains less than 4 a/o niobium.	Complex tetragonal
γ_1, γ_2	Both are bcc γ solid solutions, with differing parameters, occurring within the immiscibility loop. γ_2 would be niobium rich.	bcc
α'	Supersaturated α-like transition phase having same structure but different parameters. There is a notable contraction of the b_0 parameter as compared to the a_0 and c_0 parameters.	Orthorhombic (b_0 contraction)
α''	Supersaturated α-like transition phase having similar parameter changes as α' and, in addition, an increase in angle γ (between the a and b axes) thus resulting in a monoclinic structure.	Monoclinic (b_0 contraction) ($\angle \gamma > 90^\circ$)
γ^o	An ordered tetragonal transition phase closely related to the bcc γ phase. The structure is based on a block of $2 \times 2 \times 1$ γ cells with $c/a \lesssim 0.5$.	Tetragonal
γ_{1-2}	A bcc γ solid solution intermediate to the equilibrium γ_1 and γ_2 phases. This phase occurs during the homogeneous decomposition of γ_1 to γ_2.	bcc

---

(14) See Reference 10.

(15) See Reference 9.

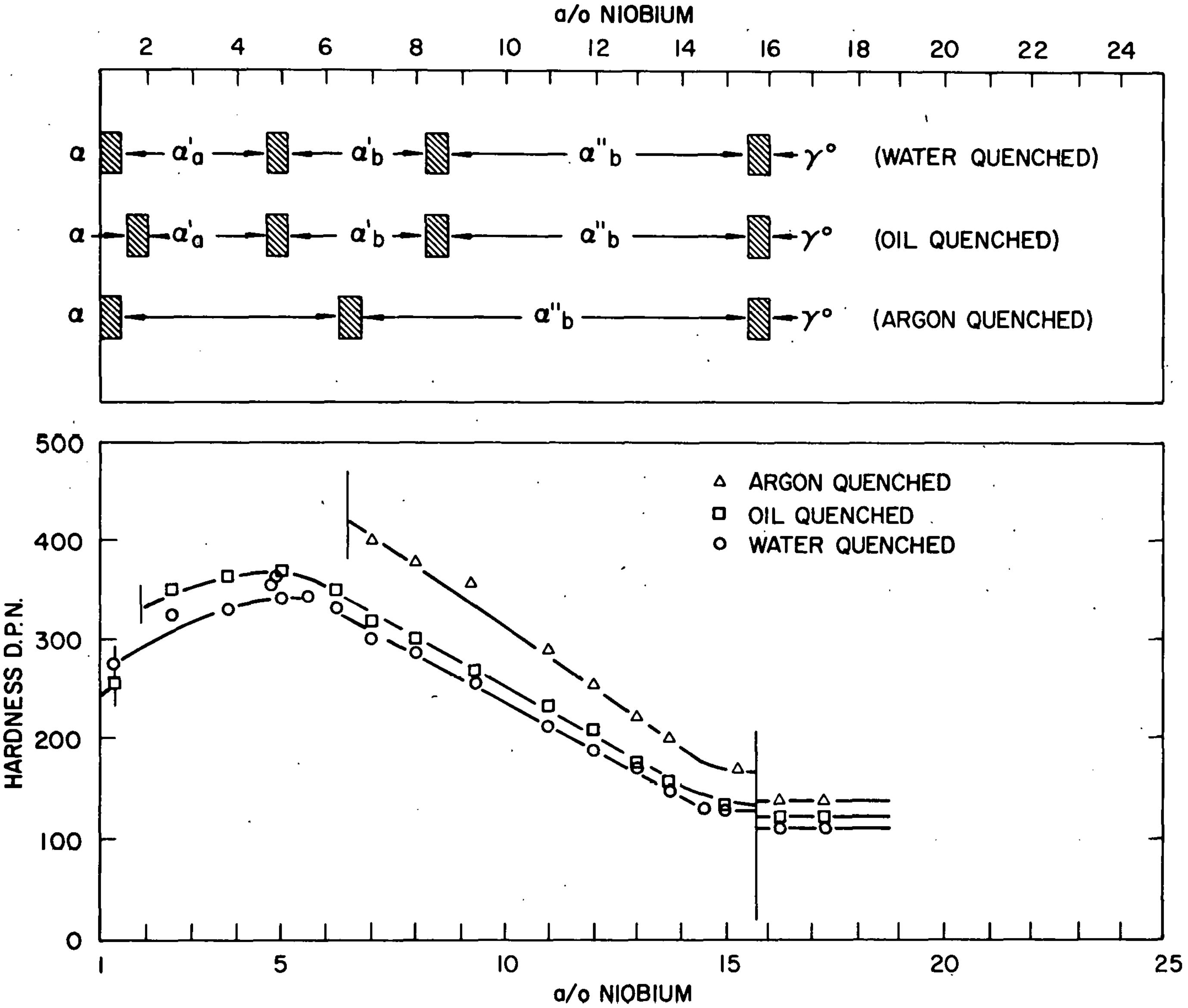

Figure 2.–Crystallographic phase (upper) and hardness (lower) as a function of composition after quenching from the gamma region. The data are from Anagnostidis.

precipitation of a niobium poor alpha uranium phase and a corresponding loss in corrosion properties.

The discontinuity in tensile and yield strengths in the vicinity of a 450°C age for the three compositions is more apparent than real. These tensile bars were brittle and often slightly bent. The combination of these two features makes true tensile loading very difficult to approximate, and hence, results in low yield and tensile strengths.

The most promising heat treatment for alloys where corrosion resistance is paramount is the low temperature heat treatment, i.e., below 350°C. At temperatures below 300°C no visible decomposition of the metastable α'' or γ° structure occurs during the one-hour aging. These alloys show a noticeable strength increase while maintaining good ductility properties.

Mechanical test data for the uranium-15 a/o niobium alloy aged for various periods of time at 150°C are shown in Figure 6. This low-temperature heat treatment results in a notable increase in yield strength and reduction in area, whereas the ultimate tensile strength and modulus decrease slightly. Thus aging at 150°C for 6 hours results in a near 50 percent increase in yield strength and a 40 percent increase in reduction of area.

The hot tensile strength data for the uranium-15 a/o

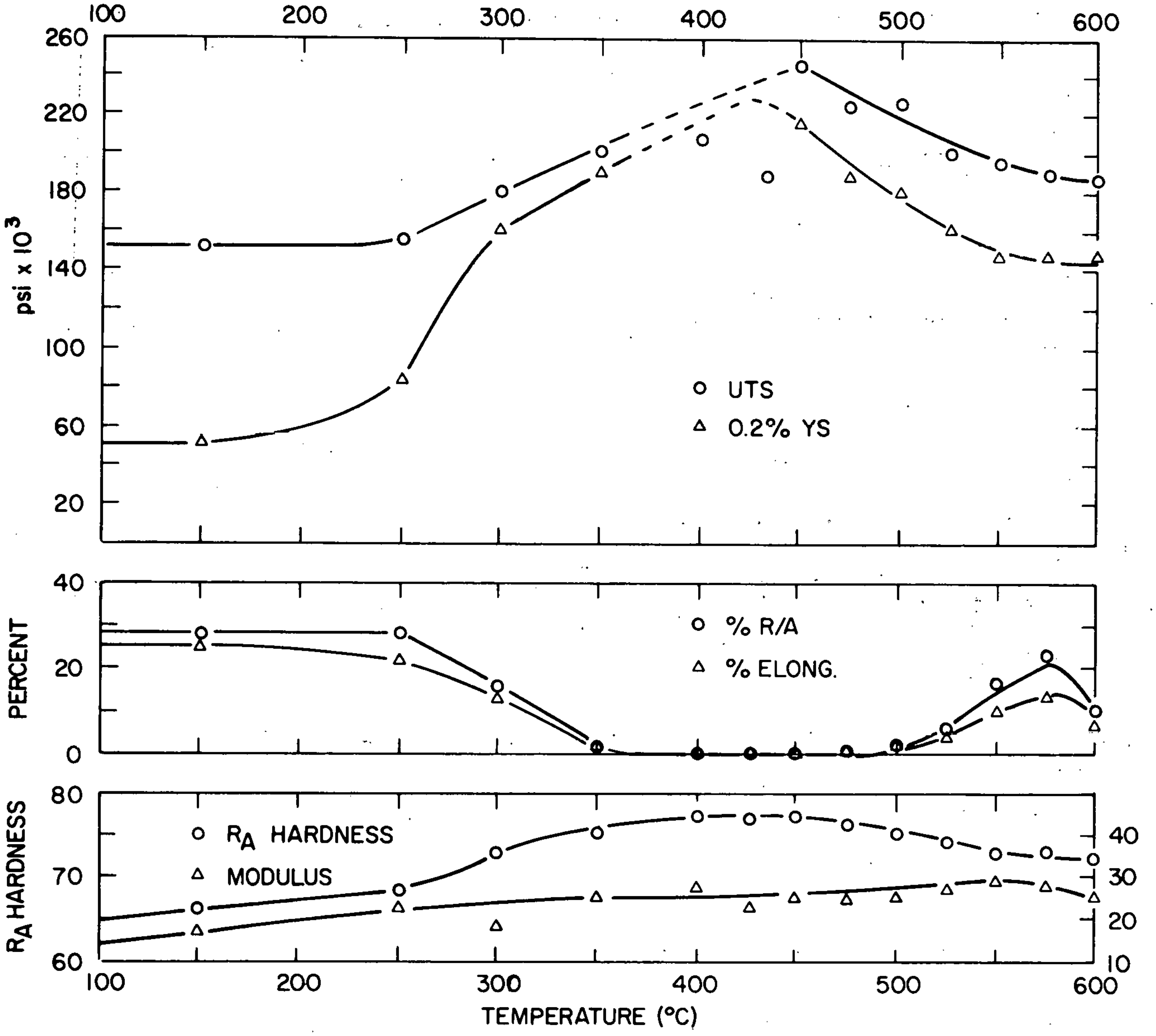

Figure 3.—Mechanical test data for the U-11 a/o Nb alloy at ambient temperatures. The samples were aged one hour at the indicated temperature and air cooled. All the samples were flat bars which were water quenched from 850°C, aged, and then machined. The blanks were cut from hot rolled, arc-cast material.

niobium alloy tested at various temperatures are shown in Figure 7. Flat bars were machined from hot rolled sheet, then solution treated 15 minutes at 850°C and water quenched. After being water quenched the samples were aged 2 hours at the indicated temperature, and then air cooled. The samples were tested at 24°, 100°, 300°, and 600°C. A decrease in tensile strength with an increase in the test temperature was noted for all heat treatments. A relation between the aging temperature and the tensile strength is also noted, with the as-quenched condition having the lowest yield strength, and the 600°C aged condition having the highest yield strength.

Supplementary mechanical test data for the uranium-11 a/o niobium and uranium-17 a/o niobium alloy are shown in Tables III and IV, respectively. Round tensile-test blanks were cut from induction-cast (previously double-arc-cast) hot-rolled bar stock. The blanks were then heated 30 minutes at 850°C and then they were water quenched. The significance of the data presented in Tables III and IV is presented in the Discussion section of this report.

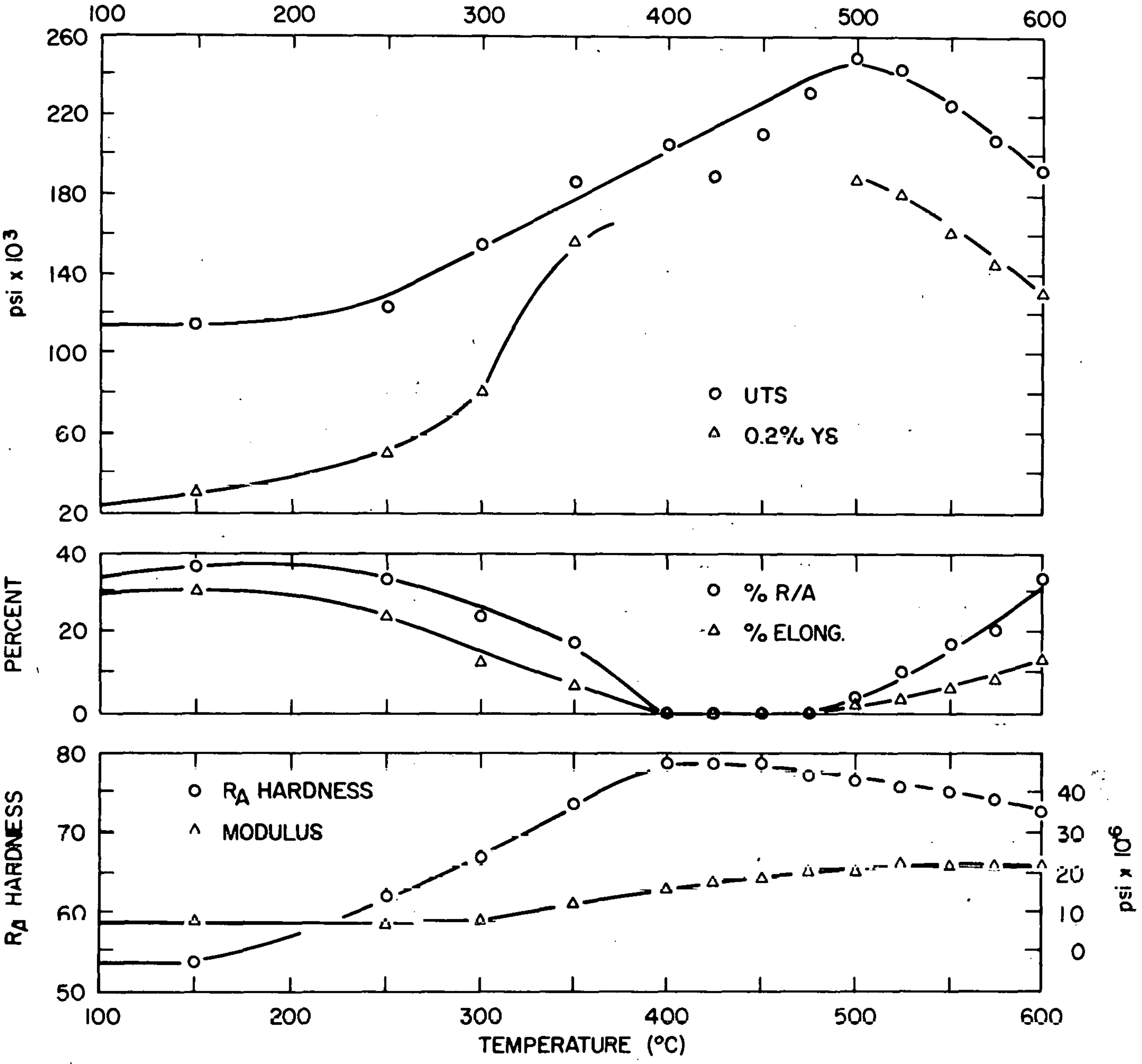

Figure 4.—Mechanical test data for the U-15 a/o Nb alloy at ambient temperatures. The samples were aged one hour at the indicated temperature and air cooled. All the samples were flat bars which were water quenched from 850°C, aged, and then machined. The blanks were cut from hot rolled, arc-cast material. The YS and UTS values for samples after water quenching from 850°C were slightly less than those shown for the 150°C age. The YS and UTS values for the samples air cooled from 850°C were 37,000 and 130,000 psi, respectively.

Metallographic and X-Ray Results.—The results of metallographic and x-ray examinations of the three principle compositions are shown in Tables V, VI and VII.

In general, x-ray examination revealed no structural change after aging for one hour below 350°C. Thus the alloys can be aged and strengthened at low temperatures (below 350°C) without any readily apparent x-ray or microstructural changes, and hence, without any large loss in corrosion resistance.

The changes in microstructure after one hour at 400°C were incomplete and resulted in diffused x-ray diffractions. After one hour at 500°C the precipitated α phase was close to equilibrium composition and gave very sharp x-ray diffractions. The accompanying γ phase had diffuse peaks and the intensity and position

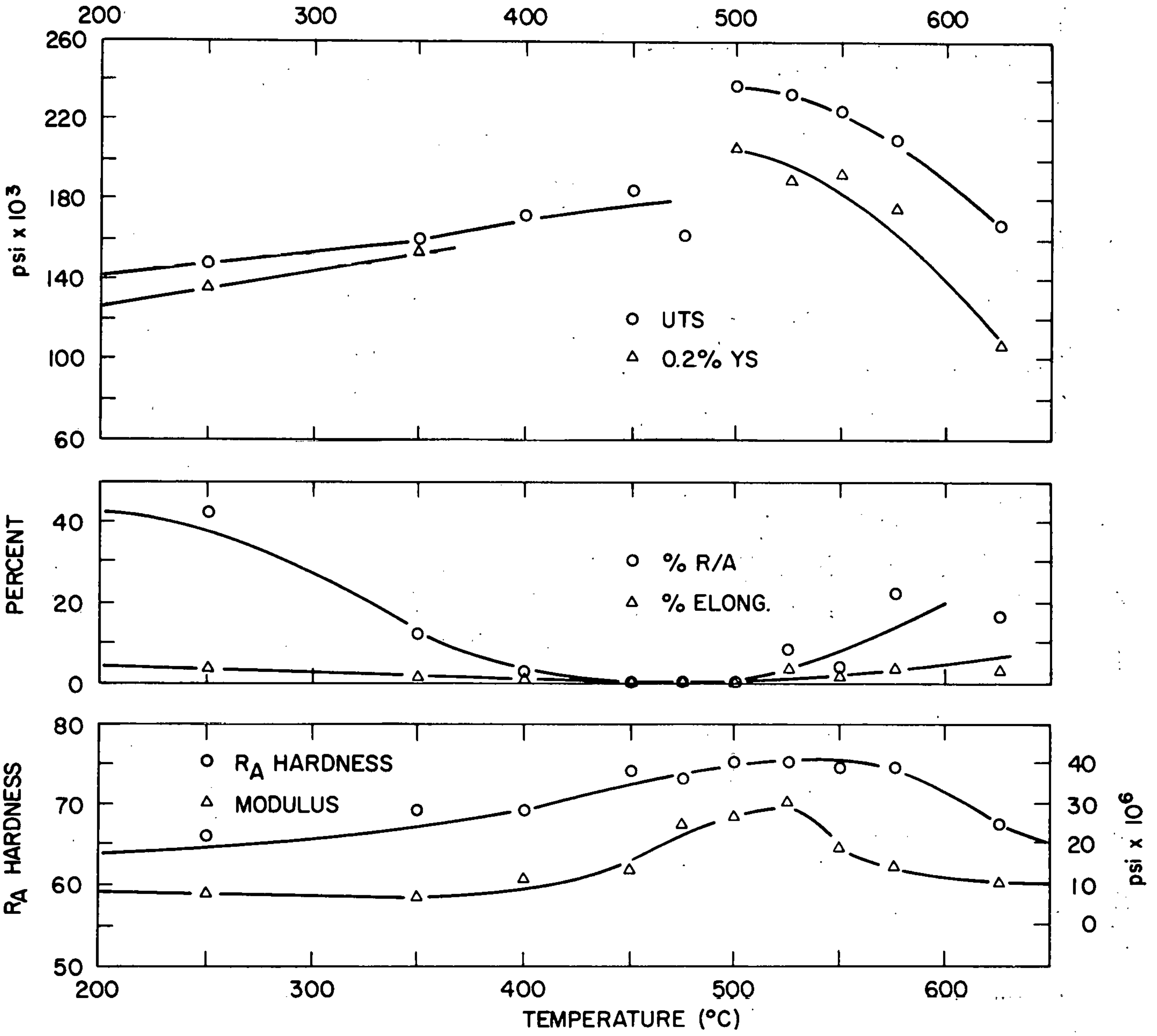

Figure 5.—Mechanical test data for the U-19 a/o Nb alloy at ambient temperatures. The samples were aged one hour at the indicated temperature and air cooled. All the samples were flat bars which were water quenched from 900°C, aged, and then machined. The blanks were cut from hot rolled, arc-cast material. The YS and UTS values for samples water quenched from 900°C were 113,000 and 125,000, respectively. The YS and UTS values for samples air cooled from 900°C were 79,000 and 125,000 psi, respectively.

of the peaks showed the matrix to be niobium poor. The alloys were closer to γ_1 in composition than they were to γ_2. Longer times at these aging temperatures would undoubtedly result in the formation of the equilibrium γ_2 phase.

The metallographic observations for the 11 a/o and 15 a/o Nb alloy agreed well with the x-ray observations. No decomposition was detected after aging for one hour at 350°C or below [See Figures 8(a) and 9(a)]. After one hour at 400°C a discontinuous precipitate formed at the grain boundaries and inclusions [Figure 9(b)]. The inclusions are primarily Nb_2C and UC. At 400°C, delineation of banding was pronounced indicating that precipitation may also occur at the band interfaces [Figure 9(b)]. At 500°C the microstructure consisted of an unresolvable matrix ($\alpha + \gamma_{1-2}$) and islands of the partially transformed metastable parent-phase [Figure 9(c)]. At 600°C the microstructure consisted entirely of the unresolvable ($\alpha + \gamma_{1-2}$) matrix. The earlier γ grain boundaries which were

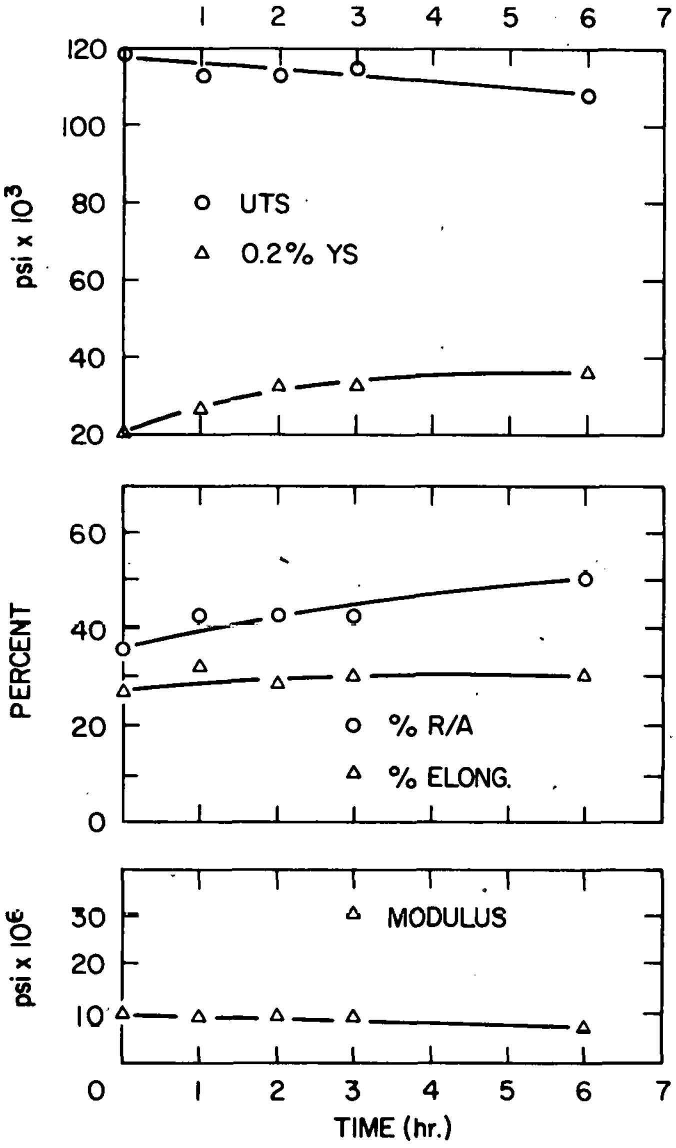

Figure 6.—Mechanical test data for the U-15 a/o Nb alloy aged at 150°C. The test was conducted at ambient temperatures. The samples were aged in oil at 150°C and air cooled. All the samples were flat bars which were water quenched from 850°C, machined, and then aged. The blanks were cut from hot rolled, arc-cast material.

observed after the lower heat treatments—aging treatments were also visible after the 500° and 600°C aging treatments.

Metallographic observations of the U-19 a/o Nb alloy were difficult to interpret. Quenching this alloy from 850°C resulted in a duplex structure consisting of light grains and dark grains. Quenching from 900°C resulted in a structure appearing to be single-phase. Aging the alloy at 250°C resulted also in a duplex structure of light grains and dark grains [Figure 10(a)]. After aging at 350° and 400°C the dark grains became progressively darker [Figure 10(b)]. It is believed that the duplex appearing structure is because of a slight niobium enrichment of certain grains at the expense of others. This would allow the niobium rich grains to be attacked by the etchant at a different rate than the niobium poor grains.

After aging at 500° and 600°C, the U-19 a/o Nb alloy appears similar to the other two compositions studied. At 500°C the microstructure consisted of an unresolvable matrix and islands of the partially transformed metastable parent-phase [Figure 10(c)]. At 600°C the microstructure consisted entirely of the unresolvable matrix.

The starting γ grain size was approximately 0.04, 0.03 and 0.02 mm for the 11, 15 and 19 a/o Nb alloys, respectively. As would be expected, no growth of the prior γ grains was observed on aging. The 11 a/o and 15 a/o Nb alloy had a uniform grain structure (Figures 8 and 9). The aged 19 a/o Nb alloy had a duplex grain structure. The light grains averaged 0.015 mm whereas the dark "grains" were about 0.03 mm in size (Figure 10).

The fractures for solution quenched specimens and specimens aged below 350°C were predominantly transcrystalline. The specimens aged for one hour at 350°C showed a mixture of transcrystalline and intercrystalline fractures. The specimens aged for one hour above 350°C had fractures that were predominantly intercrystalline. Photomicrographs showing the change from transcrystalline to intercrystalline fracture with increase in aging temperature are shown in Figures 11, 12 and 13. The change from transcrystalline to intercrystalline fracture is attributed to localized precipitation which occurs at grain boundaries after aging the specimen for one hour near 350°C.

The microhardness values at the grip area and the fracture area are shown in Tables V, VI and VII. The fracture hardness was taken at the center of the bar 60 microns from the break using a 25 gram load. A similar load was used for the grip area. As would be expected, the ductile samples showed a work hardening effect. The apparent strain softening effect for the samples aged at the higher temperatures is questionable.

Discussion

It is not surprising that the retained metastable γ^0 phase is softer than the α phase of pure uranium, even though the structure is modified from bcc. What is surprising is the extraordinary softening that occurs as the niobium content increases from 11 a/o to 15 a/o until the α'' phase is softer than pure uranium. The α'' phase is monoclinic and thus the number of

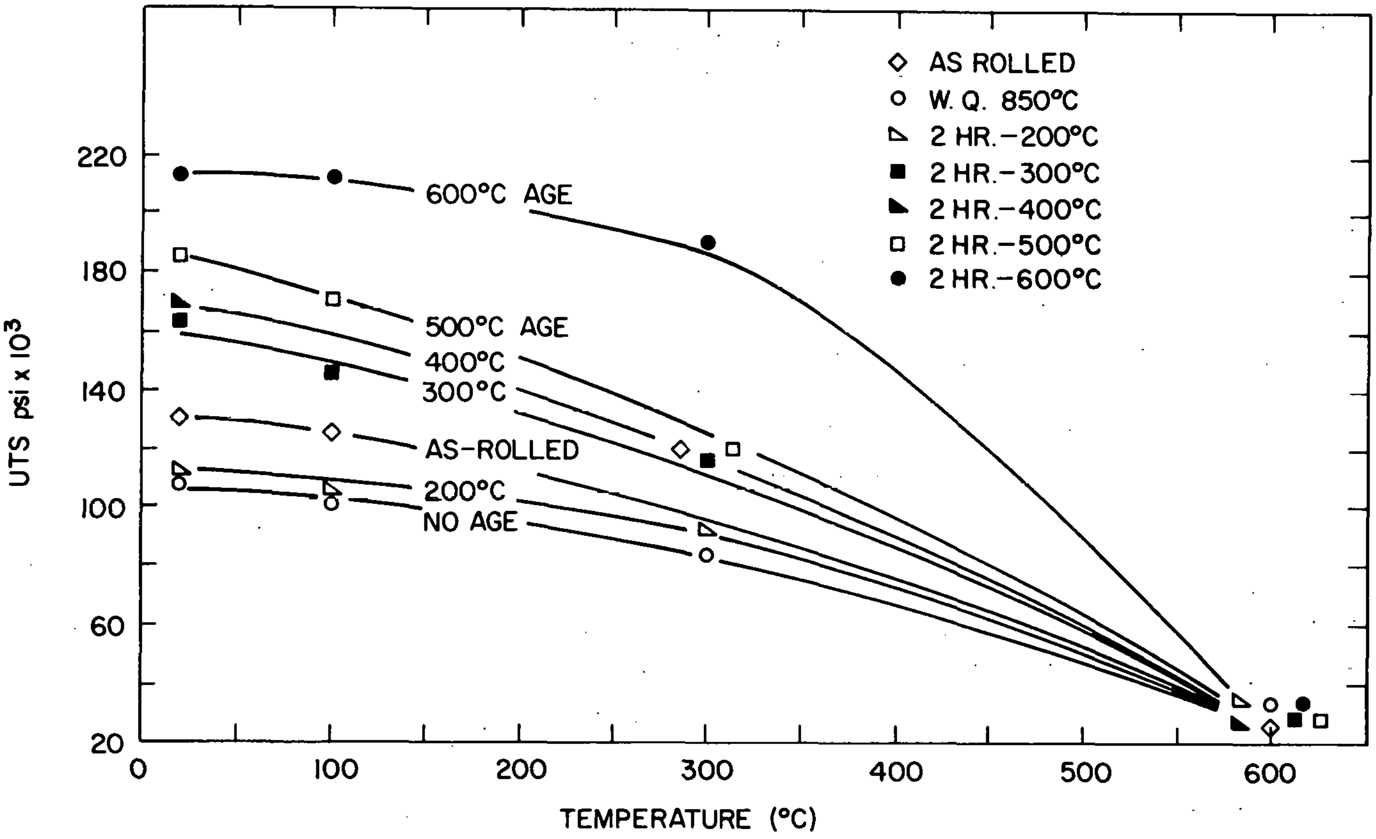

Figure 7.—Hot mechanical test data for the U-15 a/o Nb alloy. The flat bars were machined from hot rolled sheet, then solution treated 15 minutes at 850°C and water quenched. The samples were then aged 2 hours at the indicated temperature and air cooled. The samples were then tested hot at 100, 300, or 600°C. One tensile bar per data point.

TABLE III

SUPPLEMENTARY MECHANICAL TEST DATA FOR THE URANIUM-11 a/o NIOBIUM ALLOY. ROUND BLANKS WERE CUT FROM HOT-ROLLED, INDUCTION-CAST BAR STOCK. THE BLANKS WERE THEN HEATED 30 MINUTES AT 850°C AND WATER QUENCHED. TWO TENSILE BARS PER DATA POINT.

Specimen preparation	Heat treatment (°C per 1 hr)	UTS (ksi)	0.2% YS (ksi)	% R/A	% Elong. (in 1 inch)	Modulus (psi × 10^{-6})
Aged, then machined	250	159	82	26	20	14
Machined, then aged	250	159	81	27	22	14
Aged, then machined	300	195	178	20	1	18
Machined, then aged	300	172	126	24	14	16
Aged, then machined	350	178	138	19	12	17
Machined, then aged	350	197	176	3	3	19

TABLE IV

SUPPLEMENTARY MECHANICAL TEST DATA FOR THE URANIUM-17 a/o NIOBIUM ALLOY. ROUND BLANKS WERE CUT FROM HOT-ROLLED, INDUCTION-CAST BAR STOCK. THE BLANKS WERE THEN HEATED 30 MINUTES AT 900°C AND WATER QUENCHED.

Specimen preparation	Heat treatment (°C per 1 hr)	UTS	0.2% YS (ksi)	% R/A	% Elong. (in 1 inch)	E
Machined, then aged	250	127	64	46	21	6.5
Machined, then aged, 0.004 in. removed on electropolishing	250	117	55	51	31	6.5
Machined, then aged, 0.001 in. removed on electropolishing	250	117	53	52	28	6.5
Machined, then W.Q. from 850°C, then aged, light electropolish	250	118		30		

TABLE V

METALLOGRAPHIC AND X-RAY RESULTS FOR THE U-11 a/o Nb ALLOY WHOSE MECHANICAL PROPERTIES ARE SHOWN IN FIGURE 3.

History (°C)	X-ray phases	Microstructure at grip	Microstructure at fracture	D.P.N. at grip	D.P.N. at fracture
water Q. 850	α''	1-phase banded	transcrystalline, elongated grains	283	
1-hr at 150	α''	1-phase banded	transcrystalline, elongated grains	–	
1-hr at 250	α''	1-phase banded	transcrystalline, elongated grains	317	379
1-hr at 300	α''	1-phase banded	transcrystalline, elongated grains	420	376
1-hr at 350	α''	1-phase banded	trans. plus intercrystalline, no elong. grains	464	437
1-hr at 400	$\alpha'' + \gamma$ (w)	2-constituents: (α''), ($\alpha + \gamma$); ppt. at grain boundary and inclusions	intercrystalline, no elong. grains	585	572
1-hr at 500	α (s) γ_{1-2} (b)	islands in fine $\alpha + \gamma_{1-2}$ matrix	intercrystalline	503	397
1-hr at 600	α (s) γ_{1-2} (b)	fine $\alpha + \gamma_{1-2}$ matrix	intercrystalline	473	

b = broad, s = sharp, w = weak

TABLE VI

METALLOGRAPHIC AND X-RAY RESULTS FOR THE U-15 a/o Nb ALLOY WHOSE MECHANICAL PROPERTIES ARE SHOWN IN FIGURE 4.

History (°C)	X-ray phases	Microstructure at grip	Microstructure at fracture	D.P.N. at grip	D.P.N. at fracture
water Q. 850	α''	1-phase banded	transcrystalline, elongated grains	174	283
1-hr at 150	α''	1-phase banded	transcrystalline, elongated grains	–	292
1-hr at 250	α''	1-phase banded	transcrystalline, elongated grains	254	322
1-hr at 300	α''	1-phase banded	transcrystalline, elongated grains	287	376
1-hr at 350	α''	1-phase banded	trans. plus intercrystalline, no elong. grains	420	413
1-hr at 400	α'' (b) + γ_{1-2} (w,b)	some ppt. at grain boundary and inclusions, 2-constituents	intercrystalline	572	536
1-hr at 500	α (s) + γ_{1-2} (b)	islands in fine $\alpha + \gamma_{1-2}$ matrix	intercrystalline	560	525
1-hr at 600	α (s) + γ_{1-2} (b)	fine $\alpha + \gamma_{1-2}$ matrix	intercrystalline	483	446

b = broad, s = sharp, and w = weak

TABLE VII

METALLOGRAPHIC AND X-RAY RESULTS FOR THE U-19 a/o Nb ALLOY WHOSE MECHANICAL PROPERTIES ARE SHOWN IN FIGURE 5.

History (°C)	X-ray phases	Microstructure at grip	Microstructure at fracture	D.P.N. at grip	D.P.N. at fracture
air Q. 900		1-phase		–	
water Q. 900	γ^{o}	1-phase banded	transcrystalline, elongated grains	306	
1-hr at 250	γ^{o}	light and dark duplex grains	transcrystalline, elongated grains	333	283
1-hr at 350	γ^{o} (b)	light and dark duplex grains	trans. plus intercrystalline, no elong. grains	306	317
1-hr at 400	γ^{o} (b) + α (t)	light and dark duplex grains, 2 shades of dark	intercrystalline	351	297
1-hr at 500	α (s) + γ (b)	islands in fine $\alpha + \gamma_{1-2}$ matrix	intercrystalline	560	503
1-hr at 575	α (s) + γ (b)	fine $\alpha + \gamma_{1-2}$ matrix	intercrystalline	483	429

b = broad, s = sharp, t = trace, w = weak

deformation modes compared to those of pure α-uranium should be less by a factor of two. In spite of this, the α''-phase showing the largest angle of monoclinicity also shows the maximum ductility. Basinski and Christian[16] have shown that the boundaries between twinned areas of a certain type of martensitic transformation product may be very mobile, and that large deformations may be accommodated by a boundary movement to adjust the relative amounts of each type of twin. This was not observed in this work but the transformation product had, in most cases, very fine twinned areas that were not optically resolvable in an individual transformation band. In any case,

---

(16) Z. S. Basinski and J. W. Christian, *Acta Met.*, 2, 101-116 (1954).

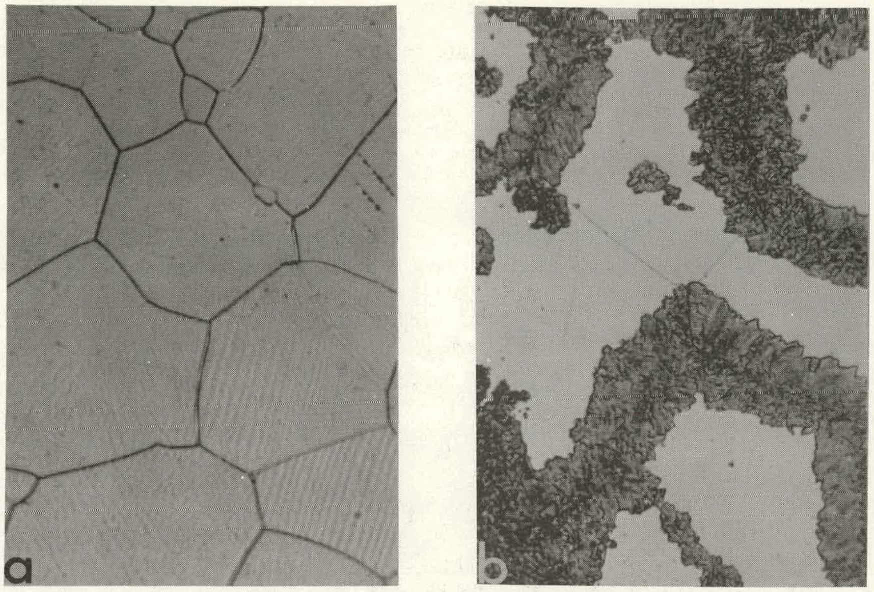

Figure 8.—Microstructures of aged U-11 a/o Nb alloys: (a) sample aged one hour at 350°C showing absence of decomposition of α'' structure, (b) sample aged one hour at 400°C showing localized precipitation at grain boundaries and inclusions. Both 500X.

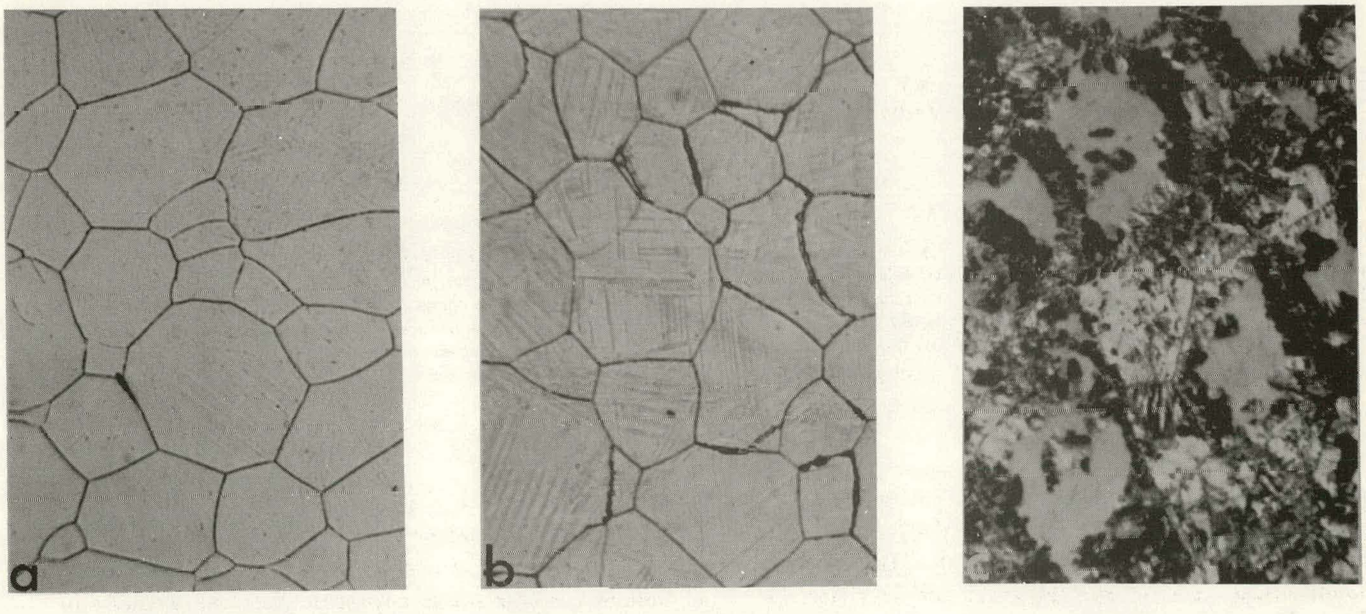

Figure 9.—Microstructures of aged U-15 a/o Nb alloys: (a) sample aged one hour at 350°C showing absence of decomposition of α'' structure, (b) sample aged one hour at 400°C showing some localized precipitation at grain boundaries and darkening of bands, (c) sample aged one hour at 500°C showing unresolvable matrix and islands of partly decomposed metastable parent phase. All 500X.

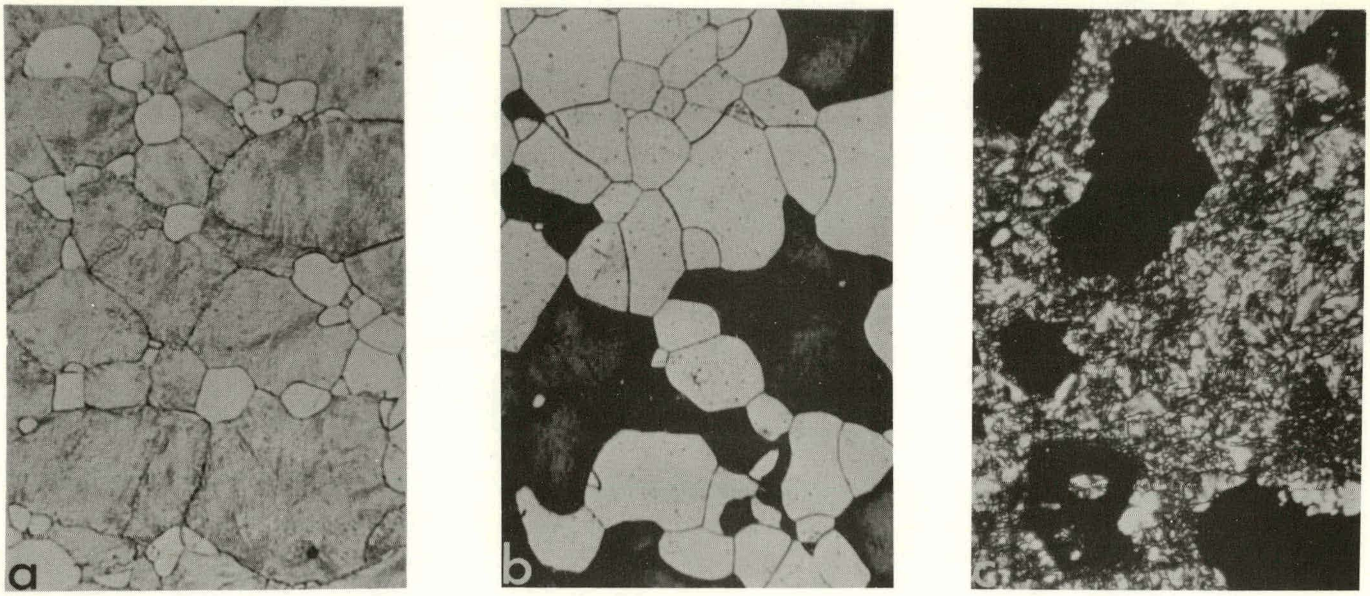

Figure 10.—Microstructures of aged U-19 a/o Nb alloys: (a) sample aged one hour at 250°C showing duplex structure, (b) sample aged one hour at 350°C showing duplex structure and darkening of grains, (c) sample aged one hour at 500°C showing unresolvable matrix and islands of partly transformed metastable parent phase under polarized light. All 500X.

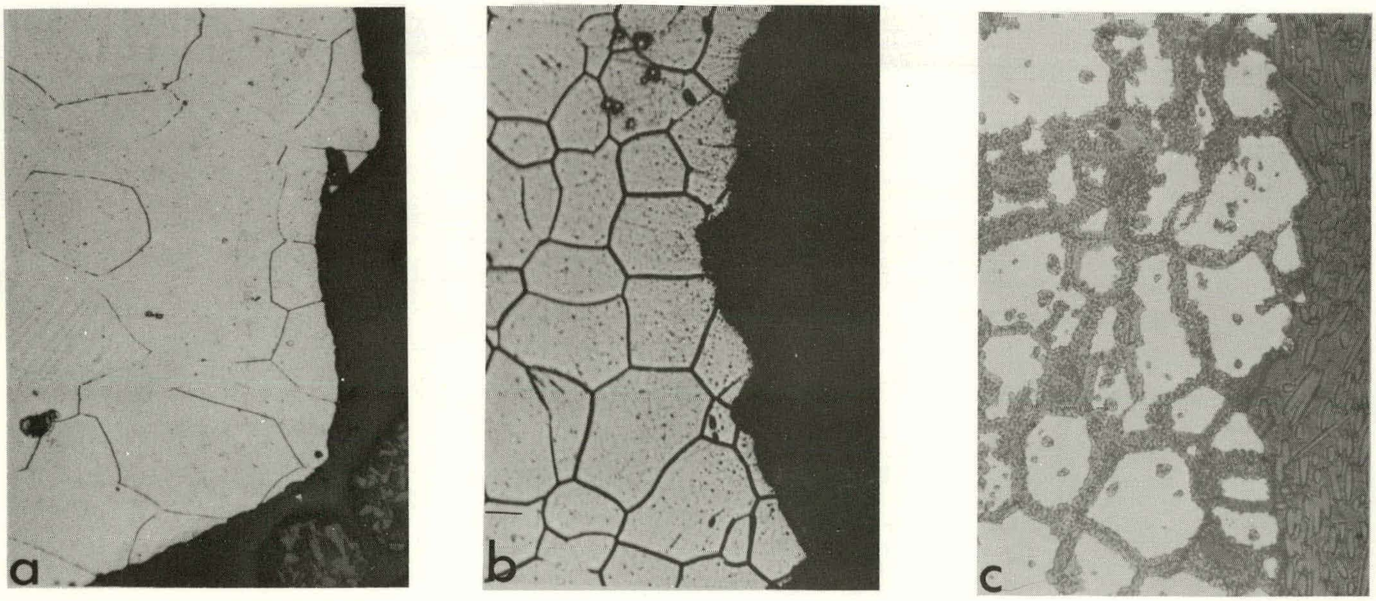

Figure 11.—Microstructures illustrating change in fracture appearance for the U-11 a/o Nb alloy with increase in aging temperature: (a) sample aged one hour at 250°C showing elongated grains and transcrystalline fracture, (b) sample aged one hour at 350°C showing mixed transcrystalline and intercrystalline fracture, (c) sample aged one hour at 400°C showing intercrystalline fracture. All 250X.

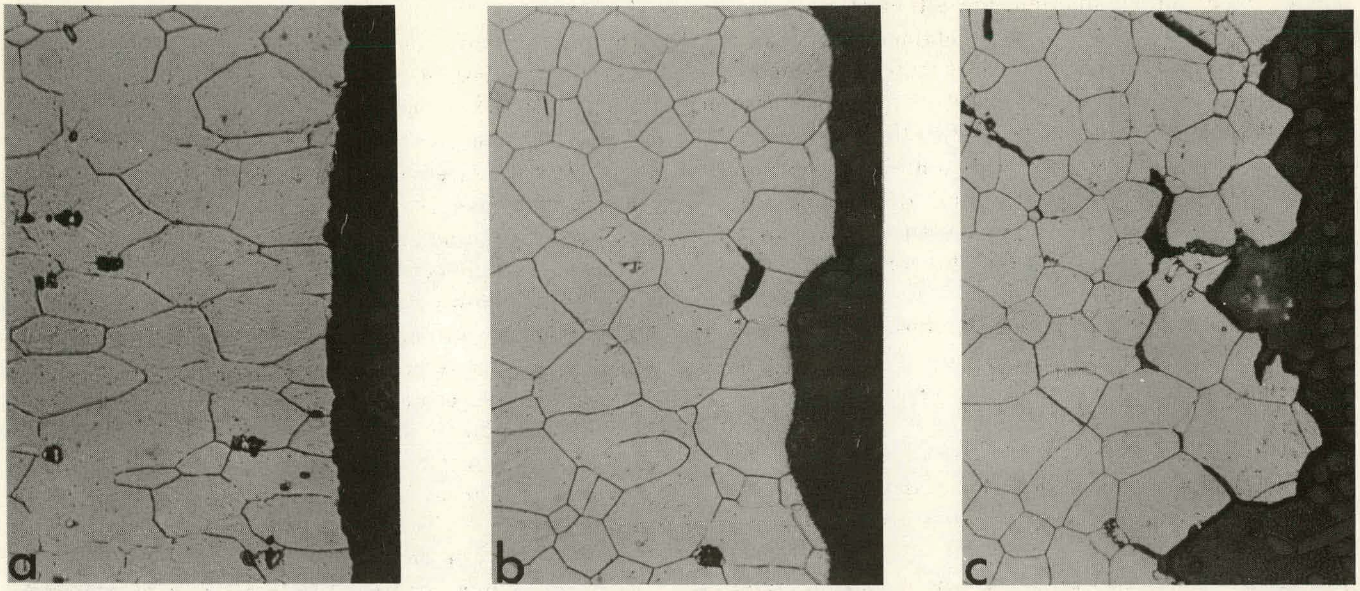

Figure 12.—Microstructures illustrating change in fracture appearance for the U-15 a/o Nb alloy with increase in aging temperature: (a) sample aged one hour at 250°C showing elongated grains and transcrystalline fracture, (b) sample aged one hour at 350°C showing mixed transcrystalline and intercrystalline fracture, (c) sample aged one hour at 400°C showing intercrystalline fracture. All 250X.

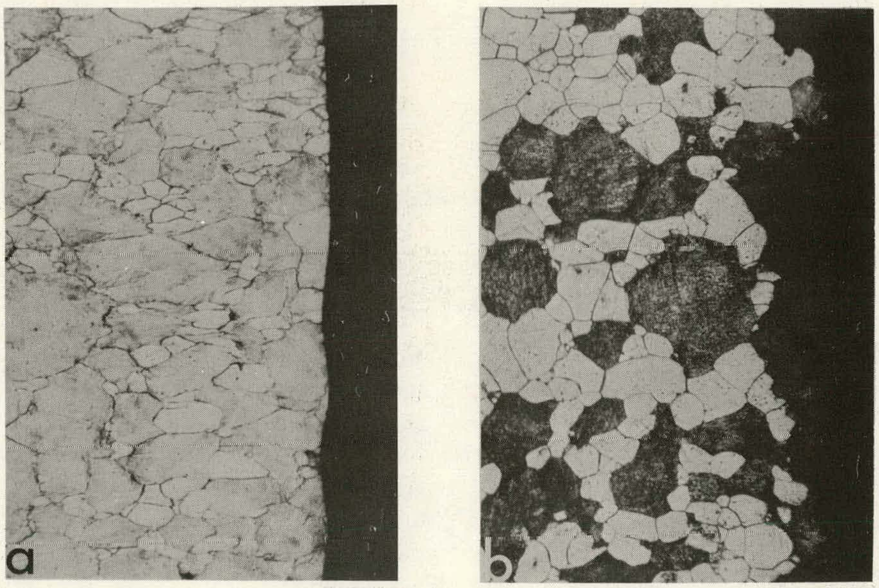

Figure 13.—Microstructures illustrating change in fracture appearance for the U-19 a/o Nb alloy with increase in aging temperature: (a) sample aged one hour at 250°C showing elongated grains and transcrystalline fracture, (b) sample aged one hour at 350°C showing mixed transcrystalline and intercrystalline fracture. All 250X.

if such a mechanism applied, the effect of niobium content would still have to be explained.

A noticeable feature shown in Figures 3, 4, and 5 is the strength minimum for the solution quenched uranium-15 a/o niobium alloy as compared to the other two compositions. The uranium-15 a/o niobium composition lies very close to the α''-γ° phase boundary (see Figure 2). When samples of this composition were entirely single-phase α'' the yield strengths averaged 30 ksi (Figure 4). It was not unusual to encounter alloys consisting of a coherent mixture of $\alpha'' + \gamma^\circ$. It is believed that these mixtures are the result of niobium micro-segregation resulting in regions where the niobium content exceeds that of the α''-γ° metastable phase boundary. The $\alpha'' + \gamma^\circ$ alloys had the lowest yield strengths and averaged 20 ksi (Figure 6). This indicates that the misfit energy between the two metastable phases must be very low.

A curious feature of the results was that the tensile strength of the martensitic α'' phase was higher in the air-quenched condition (Figure 4), whereas for the metastable γ°- phase it was higher in the water-quenched condition (Figure 5). For the metastable γ-structure, the greater degree of ordering given by rapid quenching, and the higher quenching stresses, may be responsible for the higher strengths observed. For the α'' structure, an early state of precipitation possibly occurs during the slower quench, giving rise to the greater strength. A similar behavior is observed in the uranium-molybdenum system.[17]

The increase in yield strength on aging at 150°C (Figure 6) was first noted in a uranium-7.5 a/o niobium-2.5 a/o zirconium ternary alloy and proof was presented to relate this to an ordering phenomenon.[18] A similar explanation perhaps applies for the uranium-15 a/o niobium alloy, even though a different phase is being considered, i.e., α'' as compared to γ or γ° in the ternary alloy. The diffusion of interstitial impurities at 150°C to dislocations resulting in making them less mobile could also cause an increase in yield strength.

Mechanical test data for a uranium-7.5 a/o niobium-2.5 a/o zirconium alloy has been presented elsewhere.[19,20] Certain similarities can be drawn between this ternary alloy and the uranium-niobium binary alloy. The aging trends observed in this study correlate well with those reported on the one ternary alloy.

Table III shows mechanical test data for aged uranium-11 a/o niobium alloys. It was intended to determine the strength difference for machined and then aged alloys as opposed to aged and then machined alloys. As can be seen from the data, no direct correlation is obvious.

Table IV shows that the effect of electropolishing is to lower the strength properties and increase the ductility. This is perhaps related to removal of an oxide film or a surface residual stress resulting in a dislocation sink at the surface rather than a barrier. It was also desirous to see if samples could be machined, solution quenched, then aged, and satisfactorily tested. The one test (Table IV) indicated that this could be done.

The low extensions and relatively high reductions of area that occur in the uranium-19 a/o niobium alloy (Figure 5), and in the uranium-15 a/o niobium alloy aged at various times at 150°C (Figure 6), are worthy of note. This suggests that once deformation has started, it is easier to continue deforming in that area than to initiate deformation elsewhere. It seems related to an upper yield point phenomenon, but not analogous to it, since nothing similar to Luders bands was found. It is interesting that the γ° structure is an ordered structure[21] and that the 150°C age may result in an ordered α'' structure. Thus, the severe necking may be related to a strain softening phenomenon that is a result of the ordered arrangement of atoms.

Microstructural examination revealed no evidence of circumferential cracking. At similar compositions in the uranium-molybdenum system,[22] severe circumferential cracking was observed and was attributed to stress-corrosion in air. This phenomenon has limited the use of uranium-molybdenum alloys. It is noteworthy that uranium-niobium alloys, at least in the range of study, did not show stress-corrosion cracking.

Acknowledgments.—The authors wish to acknowledge Mr. J. F. Boland for initiating this course of study and for his assistance in preparing, fabricating and heat-treating many of the specimens. Acknowledgment is also extended to Mr. W. L. Johns for aiding in the metallographic and x-ray portion of the study. The authors also wish to thank Mr. J. L. Frankeny for encouraging and supporting this research.

---

[17] R. F. Hills, B. R. Butcher, and B. W. Howlett, *J. Nucl. Materials, 11,* 149-162 (1964).

[18] C. A. W. Peterson and W. E. Elkington, "Physical and Mechanical Properties of U-7.5 Nb-2.5 Zr Alloy," Lawrence Radiation Laboratory, 1966, UCRL-14724.

[19] See Reference 18.

[20] C. A. W. Peterson and R. R. Vandervoort, "Properties of a Metastable Gamma-Phase Uranium-Base Alloy: U-7.5 Nb-2.5 Zr," Lawrence Radiation Laboratory, 1964, UCRL-7869.

[21] K. Tangri, *Memoires Scientifiques Rev. Metallurg., 58,* 469-478 (1961).

[22] See Reference 15.